

Effects of Outdoor Conditions on the Compound Parabolic Concentrator Performance

Khaled E. Albahloul
Misurata University
P.O.Box # 303, Misurata, Libya

Abstract— In this study, the effect of outdoor conditions (wind velocity and ambient temperature) on the thermal efficiency of a non-evacuated Compound Parabolic Concentrator solar collector (CPC) was investigated for two different flow rates. Matlab program was built, and simulation results for different outdoor conditions were compared with an actual outdoor data set that was taken at Misurata city, Libya. Although this study showed some effects of outdoor conditions on the CPC collector component's temperatures and heat losses, no important influence on the collector efficiency was noticed. Therefore, even though wind velocity and ambient temperature vary throughout the day, approximating them as constant values is a reasonable assumption. Mass flow rate is the most important parameter that affects the CPC efficiency.

Index Terms: CPC solar collector, thermal efficiency, outdoor conditions, heat losses.

I. INTRODUCTION

The Compound Parabolic Concentrator (CPC) has many applications in different areas like industrial heat processing, power generation, refrigeration, etc. The CPC is well suited for these applications because it provides the highest possible concentration for any angular acceptance (tracking requirement) [1]. Many papers have been published in the literature that exploring a wide range of the CPC collector designs. A steady state analysis and the mathematical model of thermal processes in a CPC collector were developed by Hsieh [2]. The effect of the variation of the system inclination on the external convective heat transfer and then the CPC overall thermal performance was done by Kothdiwala et al [3]. Fraidenraich et al. [4] considered the temperature-dependent of heat losses in their mathematical model of non-evacuated CPC solar collectors with a cylindrical receiver. Tchinda and Ngos [5] studied the effect of some of the design parameters on thermal performance of a CPC with a flat one-side receiver, and the results were compared with the experimental results.

Bansal and Sharma [6], developed a transient analysis of the tubular collector without a reflector. The analysis was extended by Chakraverty et al. [7], for the CPC collector. They developed a study of the CPC performance for time varying source input functions like solar intensity and the ambient temperature. The mass flow rate, wind velocity and solar radiation effects on the thermal performance of CPC were studied theoretically and compared with experimental data by Patel and Patel [8]. In this paper, Matlab program was built to investigate the effect of the outdoor conditions (the ambient temperature and the wind velocity) on the thermal performance of non-evacuated CPC collector at Misurata, Libya (latitude 32.41° N) for typical summer condition.

II. THE CPC SYSTEM DESCRIPTION

A schematic diagram of the used CPC in this study is shown in Fig.1. The CPC includes a compound parabolic reflecting surface whose line focus is a cylindrical Copper receiver surrounded by a glass envelope. The receiver is covered with a selective surface of high solar absorptance (α_r) and low emittance (ϵ_r) to receive energy, whilst the reflecting is an Aluminum sheeting which covered by a solar reflecting film of high reflectance (ρ_m). There is a gap between the receiver and the cusp to accommodate any deflection of the tube, and to reduce the conduction heat loss from the receiver. A transparent glass cover was fitted across the aperture to protect the reflecting film from deterioration and to reduce convective heat losses. The reflector underside was covered by insulator to reduce heat losses to the ambient.

Received 16 June, 2018; revised 29 June, 2018; accepted 31 June, 2018.

Available online Jul 3, 2018.

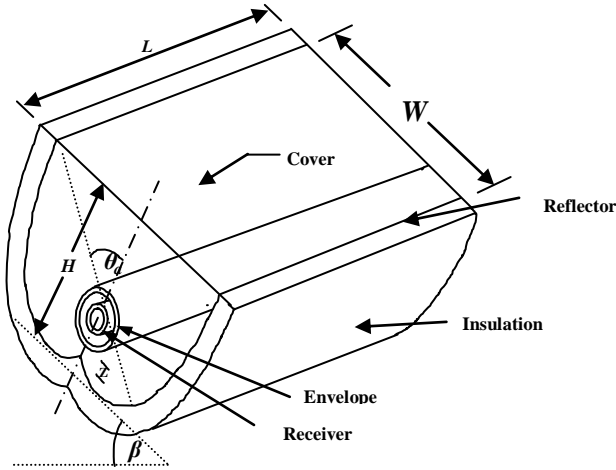


Figure 1. A Schematic Diagram of the CPC.

III. THERMAL ANALYSIS OF THE CPC COLLECTOR

Energy balance approach was used in this study, based on subdividing the medium into a number of volume elements (nodes) and then applying energy balance on each element. Nodes numbered as $i=1, 2, 3, \dots, M$. Each node has a Δx length, and during a small time interval, Δt , nodes temperatures were assumed to remain constant. one-dimensional transient heat conduction in the x -direction along the collector length, L was considered in this paper.

A. Convective heat transfer.

Convection heat transfer between working fluid and the receiver tube was calculated by

$$h_f = Nu_{r-f} \times \frac{k_f}{D_{r,i}} \quad (1)$$

where Nu_{r-f} , is Nusselt number based on $D_{r,i}$, and k_f is the working fluid thermal conductivity at T_{m1} (the bulk temperature). Nusselt number can be calculated based on flow type inside the receiver. For turbulent and transitional flow, Gnielinski [9] suggested

$$Nu_{r-f} = \frac{f/8 \times (Re - 1000) Pr_1}{1 + 12.7 \sqrt{f/8} (Pr_1^{2/3} - 1)} \left(\frac{Pr_1}{Pr_2} \right)^{0.11} \quad (2)$$

where

$$f = (1.82 \log(Re) - 1.64)^{-2} \quad (3)$$

The receiver friction factor is f , and Pr_1 and Pr_2 are Prandtl numbers evaluated at T_{m1} and at T_r respectively. For laminar flow inside pipes with a constant heat flux, flow was considered to be a fully developed and then Nu was considered to be 4.364.

Note that, contact resistance between the receiver and the fluid can be added for accuracy to calculate the total heat transfer coefficient between the receiver and

working fluid, U_{rf} . Based on receiver area, U_{rf} can be formulated as,

$$U_{rf} = \left[\frac{r_{r,o} \ln(r_{r,o}/r_{r,i})}{k_r} + \frac{A_{r,o}}{h_f A_{r,i}} \right]^{-1} \quad (4)$$

where, $r_{r,o}$ and $r_{r,i}$ are outside and inside radii of the receiver respectively, and k_r is the receiver conductivity. Outside and inside receiver areas are $A_{r,o}$ and $A_{r,i}$ respectively.

The convection heat transfer coefficient between the receiver and the envelope $h_{c,r-e}$, can be calculated based on Itoh et al. [10], which calculated for two concentric cylinders

$$h_{c,r-e} = \frac{k_{air,e} Nu_{r-e}}{r_{r,o} \ln\left(\frac{r_{e,i}}{r_{r,o}}\right)} \quad (5)$$

where, $Nu_{r-e} = 0.18 Gr_{r-e}^{0.25}$ and

$$Gr_{r-e} = \frac{g_a \beta_e (T_r - T_e) \left(r_{r,o} \ln\left(\frac{r_{e,i}}{r_{r,o}}\right) \right)^3}{\nu_e^2}$$

The gravitational acceleration is g_a , and β_e is a volumetric expansion coefficient, $\beta_e = 1/T_e$. Prandtl number was taken to be 0.71. The conductivity and kinematic viscosity were calculated from Rabl, [1,11], where

$$k_{air,e} = k_o T_e^{0.7}, \quad \nu_e = \nu_o T_e^{1.7}, \quad k_o = 4.86 \times 10^{-4} \text{ W/m. K}^{0.7},$$

$$\text{and } \nu_o = 9.76 \times 10^{-10} \text{ (m}^2/\text{s. K}^{1.7}\text{)}$$

Several experimental and theoretical studies have been done to determine convective heat transfer correlations between the envelope and the cover for CPCs. The angular dependent convective was considered in this study. Nusselt number was calculated based on Eames and Norton [12], correlation,

$$Nu_{e-c} = 0.398 \left(\frac{2H}{W} \right)^{0.365} \times \frac{Gr_{e-c}^{(0.1825+0.0736 \cos(\beta-45))}}{1.24 + 0.66054 \cos(\beta-45)} \quad (6)$$

where, W is an aperture cover width, β is the tilted angle, and H is the reflector height. Gr is Grashof number, which is calculated as

$$Gr_{e-c} = \frac{g_a \beta_a (T_e - T_c) \times (2r_{e,o})^3}{\nu_c^2} \quad (7)$$

The volumetric expansion coefficient is β_a , $\beta_a = 1/T_c$. Also, $k_{air,c} = k_o T_c^{0.7}$, and $\nu_c = \nu_o T_c^{1.7}$.

The convective heat transfer correlations between the envelope and the cover was calculated as

$$h_{c,e-c} = \frac{Nu_{e-c} \times k_{air,c}}{2 \times r_{e,o}} \quad (8)$$

The convection between the cover and atmosphere is the largest source of heat losses, and was given by Kothdiwala et al. [3]

$$h_{c,c-a} = 5.7 + 3.8V_w + 1.42 \left[\frac{(T_c - T_a) \sin \beta}{W} \right]^{0.25} \quad (9)$$

where V_w is the wind velocity

B. Radiation heat transfer.

Radiation heat transfer coefficients are given by the Stefan-Boltzmann law. The radiation heat transfer coefficient between the receiver tube and the envelope ($h_{r,r-e}$) is given by

$$h_{r,r-e} = \frac{\sigma(T_r + T_e)(T_r^2 + T_e^2)}{\frac{1}{\epsilon_r} + \frac{A_r}{A_e} \left(\frac{1}{\epsilon_e} - 1 \right)} \quad (10)$$

and the radiation heat transfer coefficient between the envelope and the cover, ($h_{r,e-c}$) is

$$h_{r,e-c} = \frac{\sigma(T_e + T_c)(T_e^2 + T_c^2)}{\frac{1}{\epsilon_e} + \frac{A_e}{A_c} \left(\frac{1}{\epsilon_c} - 1 \right)} \quad (11)$$

The cover was assumed to be a small convex gray object in a large blackbody cavity (sky). The radiation heat transfer coefficient exchanged between the cover and the sky ($h_{r,c-s}$) is simplified to:

$$h_{r,c-s} = \frac{\epsilon_c \sigma (T_c^4 - T_s^4)}{(T_c - T_a)} \quad (12)$$

Sky temperature, T_s can be related to the ground-level ambient temperature [2]

$$T_s = T_a - 6 \quad (13)$$

In the above equation, T_s and T_a are in °C.

C. The receiver energy balance.

Receiver tube was divided to number M of small elements, and for each element (i) of the receiver tube (Figure. 2), thermal energy balance can be written as

$$k_r \times \pi(r_{r,o}^2 - r_{r,i}^2) \left(\frac{T_{r,i-1}^n - T_{r,i}^n}{\Delta x} \right) + k_r \times \pi(r_{r,o}^2 - r_{r,i}^2) \left(\frac{T_{r,i+1}^n - T_{r,i}^n}{\Delta x} \right) + Q_{abs,r} - Q_{loss,r-e} - Q_u = d_r V_{r,element} C_r \left(\frac{T_{r,i}^{n+1} - T_{r,i}^n}{\Delta t} \right) \quad (14)$$

where, k_r , d_r , $V_{r,element}$, and C_r are thermal conductivity, density, volume and the specific heat of receiver, respectively. Note, $V_{r,element} = \pi(r_{r,o}^2 - r_{r,i}^2) \times \Delta x$.

The heat losses (convection and radiation) from the receiver element to the envelope, $Q_{loss,r-e}$ which is given by

$$Q_{loss,r-e} = h_{c,r-e} (2\pi r_{r,o} \Delta x) (T_{r,i}^n - T_{e,i}^n) + h_{r,r-e} (2\pi r_{r,o} \Delta x) (T_{r,i}^n - T_{e,i}^n) \quad (15)$$

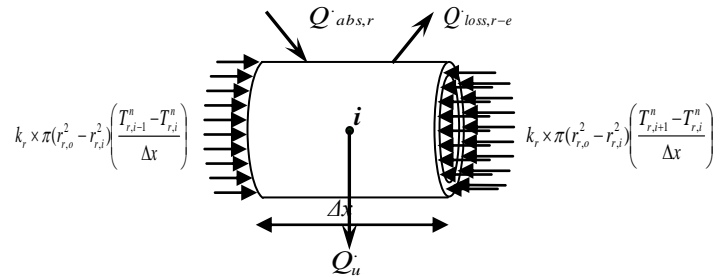


Figure 2. Discrete Element in the Receiver Tube.

Solar radiation (beam and diffuse) absorbed by the receiver, $Q_{abs,r}$ is given by

$$Q_{abs,r} = (q_{b,r} + q_{d,r}) \times 2\pi r_{r,o} \Delta x \quad (16)$$

Based on a unit receiver area, the beam and diffuse radiation absorbed by the receiver are $q_{b,r}$, $q_{d,r}$ respectively, which are calculated based on Hsieh [2].

Q_u is the useful heat transferred to the working fluid,

$$Q_u = U_{fj} (2\pi r_{r,i} \Delta x) (T_{r,i}^n - T_{f,i}^n) \quad (17)$$

Temperatures of receiver, working fluid, and the envelope for this element i at time n are $T_{r,i}^n$, $T_{f,i}^n$, $T_{e,i}^n$, respectively.

By solving Eq. 14 for the new receiver temperature $T_{r,i}^{n+1}$, the following formula can be obtained

$$T_{r,i}^{n+1} = a_1 \Delta t (q_{b,r} + q_{d,r}) + b_1 \Delta t T_{r,i+1}^n + b_1 \Delta t T_{r,i-1}^n + c_1 \Delta t T_{e,i}^n + d_1 \Delta t T_{f,i}^n + (1 - (2b_1 + c_1 + d_1) \Delta t) T_{r,i}^n \quad (18)$$

where, $a_1 = \frac{2r_{r,o}}{d_r C_r (r_{r,o}^2 - r_{r,i}^2)}$, $b_1 = \frac{k_r}{d_r C_r \Delta x^2}$,
 $c_1 = \frac{2r_{r,o}(h_{c,r-e} + h_{r,r-e})}{d_r C_r (r_{r,o}^2 - r_{r,i}^2)}$, $d_1 = \frac{2r_{r,i}U_{ff}}{d_r C_r (r_{r,o}^2 - r_{r,i}^2)}$

Equation 18 is a general relation for each interior node of a receiver, but this relation is not applicable for the boundaries nodes. By applying the energy balance for the boundary nodes, and considering adiabatic boundary conditions for these elements, Eq. 18 can be written for the first and the last control volumes ($i=1$, and $i=M$), as,

$$T_{r,1}^{n+1} = a_1 \Delta t (q'_{b,r} + q'_{d,r}) + 2b_1 \Delta t T_{r,2}^n + c_1 \Delta t T_{e,1}^n + d_1 \Delta t T_{f,1}^n + (1 - (2b_1 + c_1 + d_1) \Delta t) T_{r,1}^n \quad (19)$$

and

$$T_{r,M}^{n+1} = a_1 \Delta t (q'_{b,r} + q'_{d,r}) + 2b_1 \Delta t T_{r,M-1}^n + c_1 \Delta t T_{e,M}^n + d_1 \Delta t T_{f,M}^n + (1 - (2b_1 + c_1 + d_1) \Delta t) T_{r,M}^n \quad (20)$$

Note that the length of these control volumes are $(\Delta x/2)$.

D. The working fluid energy balance.

The problem was assumed to be one dimension and transient, so, the thermal energy balance for each fluid element (see Fig. 3) is

$$m \dot{C}_f T_{f,i-1}^n - m \dot{C}_f T_{f,i}^n + \dot{Q}_u = d_f V_{f,element} C_f \left(\frac{T_{f,i}^{n+1} - T_{f,i}^n}{\Delta t} \right) \quad (21)$$

where, d_f , C_f , m and $V_{f,element}$ are density, specific heat, flow rate, and volume of the working fluid element respectively. Note, $V_{f,element} = \pi r_{r,i}^2 \times \Delta x$.

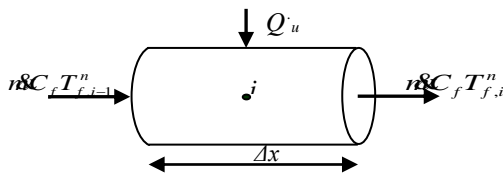


Figure 3. Energy Balance for the Working Fluid.

By solving Eq. 21 for the new fluid temperature,

$$T_{f,i}^{n+1} = a_2 \Delta t T_{r,i}^n + b_2 \Delta t T_{f,i-1}^n + (1 - (a_2 + b_2) \Delta t) T_{f,i}^n \quad (22)$$

where, $i=2,3,\dots,M$, $a_2 = \frac{2U_{ff}}{d_f C_f r_{r,i}}$, $b_2 = \frac{m \dot{C}_f}{d_f \pi r_{r,i}^2 \Delta x}$

Because T_{in} was considered to be constant at any time, the inlet boundary condition for the first control volume is $T_{f,1}^n = T_{in}$.

Similarly, the new envelope temperature $T_{e,i}^{n+1}$, and the new cover temperature $T_{c,i}^{n+1}$ for this element are given by

$$T_{e,i}^{n+1} = b_3 \Delta t (q'_{b,e} + q'_{d,e}) + c_3 \Delta t T_{r,i}^n + (d_3 + e_3) \Delta t T_{c,i}^n + (1 - (c_3 + d_3 + e_3) \Delta t) T_{e,i}^n \quad (23)$$

$$T_{c,i}^{n+1} = a_4 \Delta t (q'_{b,c} + q'_{d,c}) + (c_4 + d_4) \Delta t T_{e,i}^n + e_4 \Delta t T_a + f_4 \Delta t T_s + (1 - (c_4 + d_4 + e_4 + f_4) \Delta t) T_{c,i}^n \quad (24)$$

where, $a_3 = \frac{2}{d_e C_e (r_{e,o}^2 - r_{e,i}^2)}$, $b_3 = a_3 r_{r,o}$,

$$c_3 = b_3 (h_{c,r-e} + h_{r,r-e}), \quad d_3 = a_3 r_{e,o} h_{r,e-c}, \quad e_3 = a_3 r_{e,o} h_{c,e-c}$$

$$a_4 = \frac{2\pi r_{r,o}}{d_c C_c t_c W}, \quad b_4 = \frac{2\pi r_{e,o}}{d_c C_c t_c W}, \quad c_4 = b_4 h_{c,e-c}$$

$$d_4 = b_4 h_{r,e-c}, \quad e_4 = \frac{h_{c,c-a}}{d_c C_c t_c}, \quad f_4 = \frac{h_{r,c-s}}{d_c C_c t_c}$$

Beam and diffuse radiations that absorbed by the envelope and cover based on a unit receiver area are $q'_{b,e}$, $q'_{d,e}$, $q'_{b,c}$, and $q'_{d,c}$ respectively, calculated using suggestions from Hsieh [2].

Note that, the conduction heat transfer between the elements was neglected due to the low thermal conductivities of the envelope and cover (glass).

Based on unit receiver area, the overall heat losses coefficient, U_l can be calculated as,

$$U_l = \frac{1}{A_r} \left[\frac{1}{(h_{c,r-e} + h_{r,r-e}) A_r} + \frac{1}{(h_{c,e-c} + h_{r,e-c}) A_e} + \frac{1}{(h_{c,c-a} + h_{r,c-s}) A_c} \right]^{-1} \quad (25)$$

E. The CPC efficiency.

The total useful energy collected from the CPC collector, \dot{Q}_u and which is extracted in the form of heat by working fluid, can be written as

$$\dot{Q}_u = m \dot{C}_f (T_o - T_i) \quad (26)$$

where, T_i and T_o , are the inlet and outlet fluid temperatures respectively, and m is the fluid flow rate. The instantaneous efficiency of a collector, η_c can be defined as,

$$\eta_c = \frac{\dot{Q}_u}{I_t \times A_c} \quad (27)$$

where, I_t is the total (beam and diffuse) incident radiation on aperture plane, which is calculated using ASHRAE method for Misurata city in Libya.

IV. RESULTS AND DISCUSSIONS

Matlab program was built to analyze the CPC solar collector performance under outdoor conditions. The results that will be presented in this section are for a fixed orientation mode ($E-W$ orientation of the longitudinal axis of the CPC). The CPC has a concentration ratio, $C = 2$, and a fixed tilted angle at the longitude angle. This study was performed under two different working fluid flow rates, $m=0.001\text{kg/s}$, and $m=0.01\text{kg/s}$ (**Note:** plotted on the figures are two sets of results, the lower is for $m=0.01\text{kg/s}$ and the other is for $m=0.001\text{kg/s}$). The daily collected period was eight hours. The CPC dimensions and properties in this simulation are shown in Table 1.

The effects of wind velocity and ambient temperature on heat fluxes, component's temperatures, and the CPC efficiency were investigated. Results obtained using different constant values of wind velocity and ambient temperature during the collected period were compared with the results that computed from the actual data (using measured values). The selected day for this study was June 21st. Wind velocity and ambient temperature distributions during this day are indicated in Figure. 4 (solid line is ambient temperature and symbols are for wind velocity, V_w).

Table 1.The CPC Dimensions and Properties.

$L = 2\text{ m}$	$k_r = 385\text{W/m.K}$	$t_c = 0.004\text{m}$	$\rho_m = 0.85$	$\tau_c = \tau_e = 0.90$
$r_{r,i} = 0.019\text{m}$	$k_c = k_e = 1.05\text{W/m.K}$	$C_c = C_e = 820\text{J/kg.}^\circ\text{K}$	$\rho_r = 0.15$	$\alpha_c = \alpha_e = 0.05$
$r_{r,o} = 0.02\text{ m}$	$C_r = 383.1\text{ J/kg.}^\circ\text{K}$	$\varepsilon_c = \varepsilon_e = 0.85$	$\varepsilon_r = 0.05$	$d_r = 8954\text{ kg/m}^3$
$r_{e,i} = 0.026\text{ m}$	$r_{e,o} = 0.027\text{ m}$	$\rho_c = \rho_e = 0.05$	$\alpha_r = 0.95$	$d_c = d_e = 2707\text{kg/m}^3$

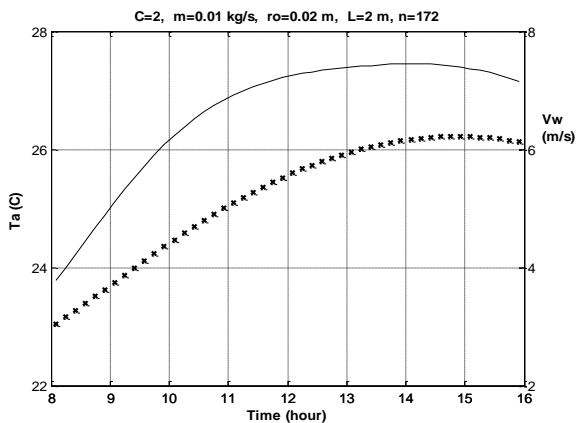


Figure 4. Wind Velocity and Ambient Temperature Distributions on 21/6 in Misurata

Simulation results in Figures. 5, and 6 showed some influence of wind velocity and ambient temperature on the heat losses from the cover to surrounding (convection and radiation respectively). Increasing wind velocity leads to increase convection heat transfer coefficient (convection heat losses from cover), which decreases the cover temperature (see Figure. 7). Due to the dependence of radiation on temperature, radiation heat losses decrease as well, Figure. 6.

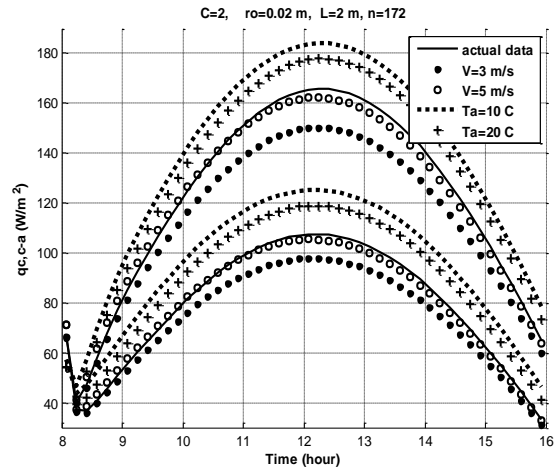


Figure 5. The Outdoor Condition Effect on Convection Heat Transferred between Cover and Ambient.

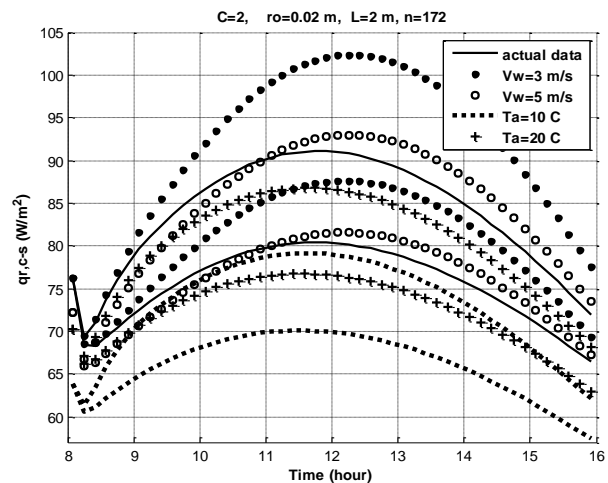


Figure 6. The Outdoor Condition Effect on Radiation Heat Transferred between Cover and Ambient.

On the other hand, ambient temperature has a reversed behavior on these losses. Increasing the ambient temperature leads to decrease the temperature difference, and this reduces the convection heat transfer rate.

Note that, actual data in the figures refers to the simulation results that used the actual outdoor conditions for Misurata. By comparing these actual results with that obtained assuming wind velocity as a constant value ($V_w=5\text{m/s}$) throughout the day, no important differences can be seen (see Figures. 5, 6, and 7).

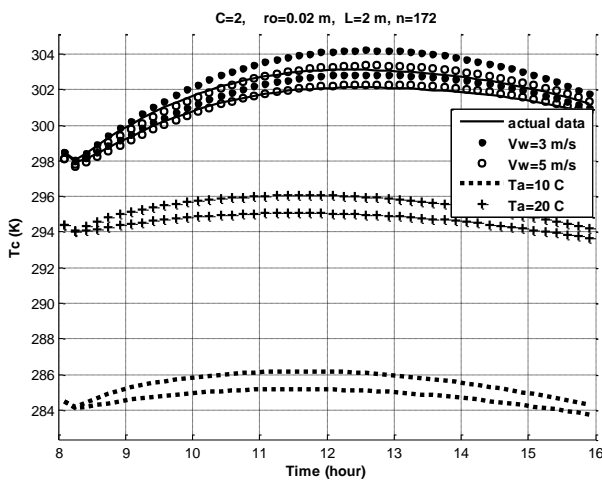


Figure 7. The Outdoor Conditions Effects on the Cover Temperature.

Figures (8, 9) show similar behavior for the convection and radiation energy exchanged between the envelope and cover. However, wind velocity effect is less important here than the ambient temperature effect, especially with high flow rate case.

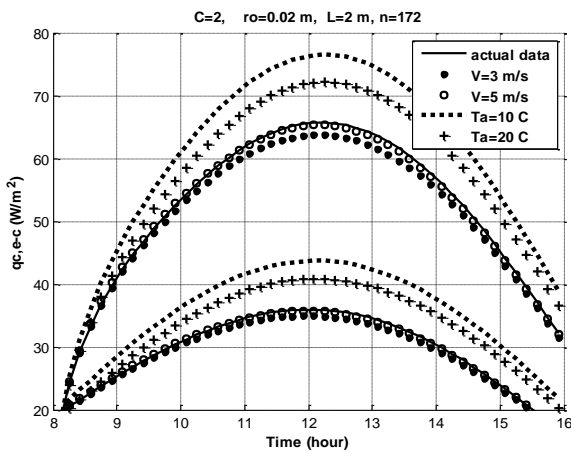


Figure 8. The Outdoor Condition Effect on Convection Heat Transferred between Envelope and Cover.

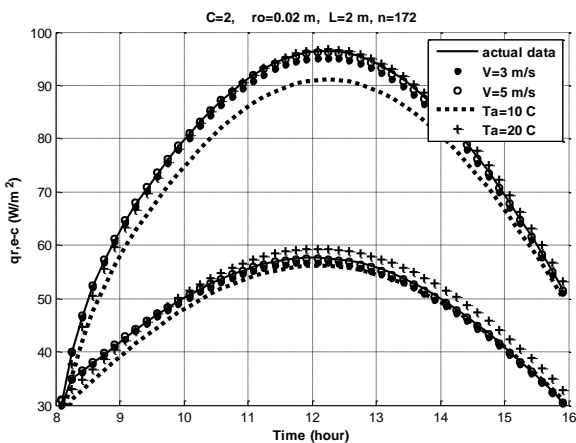


Figure 9. The Outdoor Condition Effect on Radiation Heat Transferred between Envelope and Cover.

The heat losses from the receiver to the envelope is affected by the variations of outdoor conditions as well. While this effect can be seen for the wind velocity, there is almost no influence for the ambient temperature. Radiation heat loss is small due to the use of the high optical properties for receiver, and that suppresses the radiation losses, see Figures. 10, and 11. These effects on heat losses reflect on receiver's temperature, see Figure.12.

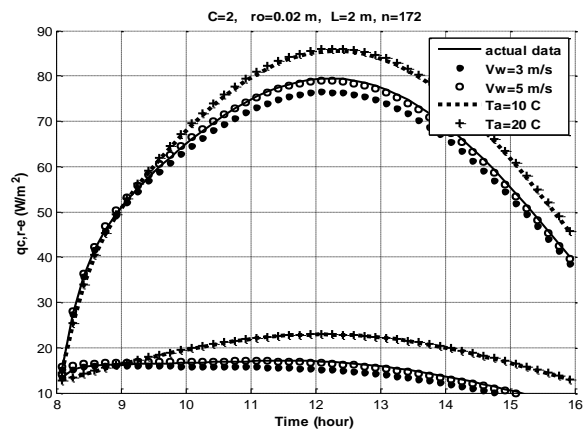


Figure 10. The Outdoor Condition Effect on Convection Heat Transferred between Receiver and Envelope.

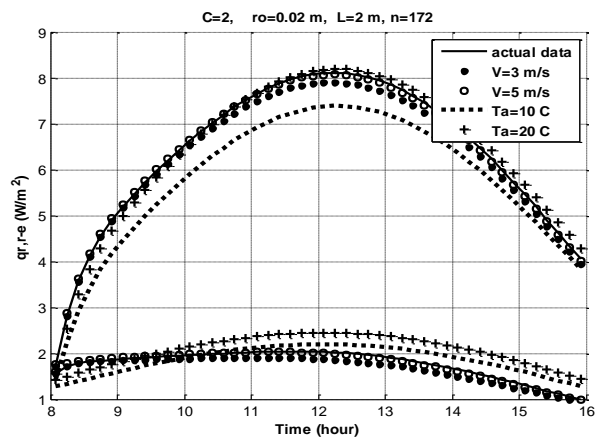


Figure 11. The Outdoor Condition Effect on Radiation Heat Transferred between Receiver and Envelope.

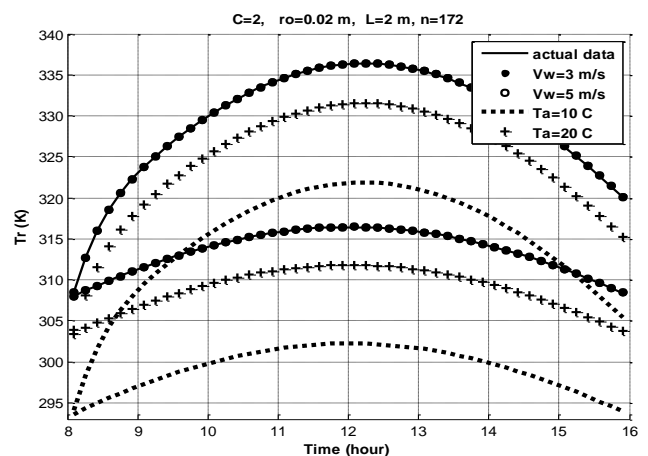


Figure 12. The Outdoor Conditions Effects on the Receiver Temperature.

In all the presented simulation results (except on the cover temperature), the important effect of the flow rate on heat losses (especially its effect on the convection parts), and then component's temperatures can be seen. Heat transfer coefficient between the receiver and the working fluid will increase with increasing the flow rate and then reduces the receiver temperature.

The total effect of outdoor conditions on the CPC system heat losses can be represented by the overall heat losses coefficient, Figure. 13. Its value increases with increases wind velocity due to increasing the convection heat losses which is dominant relative to the radiation losses. Its value increases with increasing the outdoor conditions, but the important effect is for the flow rate.

Finally, due to the relatively small effect of the outdoor conditions on the system heat losses, their effects on the CPC efficiency throughout the day were small, see Figure. 14. The obvious effect on the efficiency is due to the flow rate. The CPC efficiency is approximately constant throughout the day at large flow rate (45-47%), but it varies throughout the day in a small flow rate case. That is due to the stability for the heat losses at high flow rate case. Even though the maximum losses value at noon due to the maximum solar intensity, the heat gain increases and then the system efficiency.

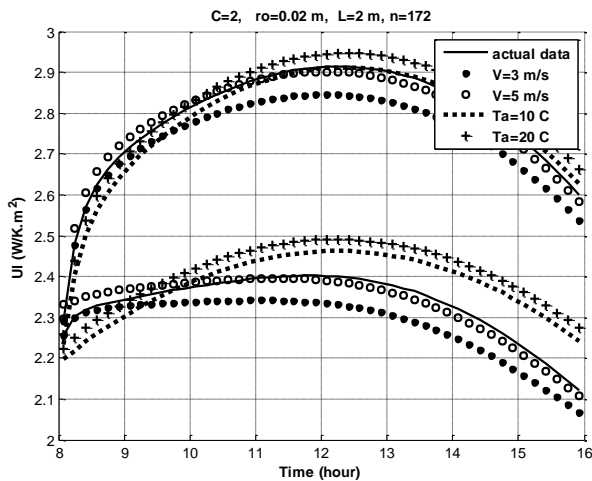


Figure 13. The Outdoor Condition Effects on the Overall Heat Transfer Coefficient.

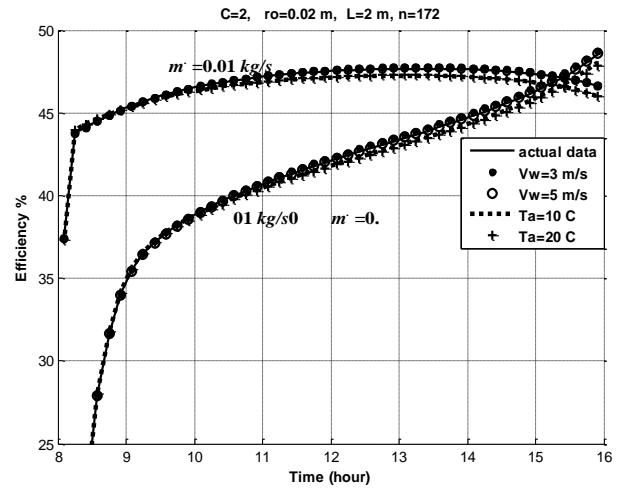


Figure 14. The Outdoor Condition Effects on the Efficiency.

V. CONCLUSIONS

Matlab program was built to investigate the influence of outdoor conditions influence (the ambient temperature and wind velocity) on the thermal performance of a non-evacuated CPC collector at two different flow rates. These results were compared with the results that obtained using the actual outdoor data. Further, the simulation results showed that:

- The effect of wind velocity on the CPC system heat losses, and component's temperatures was obvious, especially on the cover. Regarding the effect of ambient temperature, there is an equally parallel increase by almost 10 °C. However, there is no important effect on the system efficiency from both of these outdoor conditions parameters.
- Even though the actual wind velocity and the ambient temperature varying during the day, considering the average values throughout the day for these parameters is a reasonable approximation.
- The most important parameter that affects the CPC thermal efficiency is the mass flow rate.
- Due to the small effect of the outdoor conditions on the non-evacuated CPC system efficiency, and based on the economic point of view, there is no necessity to evacuate the system under these conditions.

Nomenclature

Greek letters

α	absorptivity, (<i>dimensionless</i>)
ρ	reflectivity, (<i>dimensionless</i>)
ν	kinematic viscosity, (m^2/s)
η_c	instantaneous efficiency, (<i>dimensionless</i>)
ε	emissivity, (<i>dimensionless</i>)
β	tilted angle, (Degree)
β	coefficient of volumetric expansion, ($^{\circ}K^{-1}$)
σ	constant of Stefan-Boltzmann, $W/m^2 \cdot K^4$
τ	transmittance, (<i>dimensionless</i>)

Subscripts

a	ambient
air	air
abs	absorbed
b	beam component
c	cover, convection
d	diffuse component
e	envelope
f	fluid
i	inside, inlet
$loss$	loss
m	mirror, mean
o	outside
r	receiver, radiation
s	sky
t	total
u	useful

A	area (m^2)
C	concentration ratio, specific heat ($J/kg \cdot ^{\circ}K$)
d	density (kg/m^3)
D	diameter, (m)
f	friction factor for the receiver inner surface
g_a	gravitational acceleration (m/s^2)
Gr	Grashof number, (<i>dimensionless</i>)
h	heat transfer coefficient ($W/m^2 \cdot ^{\circ}K$)
H	reflector height (m)
I	incident radiation (W/m^2)
k	thermal conductance ($W/m \cdot ^{\circ}K$)
L	collector length (m)
\dot{m}	mass flow rate (kg/s)
M	number of nodes
Nu	Nusselt number, (<i>dimensionless</i>)
Pr_1	Prandtl number at T_m , (<i>dimensionless</i>)
Pr_2	Prandtl number at T_r , (<i>dimensionless</i>)
q	heat flux based on receiver area (W/m^2)
Q	heat transfer rate, (W)
r	radius (m)
Re	Reynolds number, (<i>dimensionless</i>)
t	thickness, (m)
T	temperature ($^{\circ}K$)
Δt	time interval (sec)
U_i	overall heat losses coefficient ($W/m^2 \cdot ^{\circ}K$)
U_{σ}	total heat transfer coefficient between receiver and working fluid ($W/m^2 \cdot ^{\circ}K$)
V	volume (m^3)
V_w	wind velocity (m/s)
W	aperture cover width (m)
Δx	the nodal spacing (m)

REFERENCES

- [1] Rabl A., Optical and thermal properties of compound parabolic concentrators. *Solar Energy*, 18, 497, (1976).
- [2] Hsieh C.K., Thermal analysis of CPC collectors. *Solar Energy*, 27, pp.19–29, (1981).
- [3] Kothdiwala A. F., Norton B. and Eames P.C., The effect of variation of angle of inclination on the performance of low-concentration-ratio compound parabolic concentrating solar collectors. *Solar Energy*, 55, 301 (1995).
- [4] Fraidenraich N, Lima R.DEC.F.DE, Tiba C., and Barbosa E.M. DES., Simulation model of collector with temperature dependent heat loss coefficient. *Solar Energy*, 65, pp. 99–110, (1999).
- [5] Tchinda R. and Ngos N., A theoretical evaluation of the thermal performance of CPC with flat one-sided absorber. *Heat and Mass transfer*, 33, pp.709-718, (2006).
- [6] Bansal N.K. and Sharma A.K., Transient theory of a tubular solar energy collector. *Solar Energy*, 32, 67 (1984).
- [7] Chakraverty S., Bansal N.K. and Garg H.P., Transient analysis of a CPC collector with time dependent input function. *Solar Energy*, 38, 179 (1987).
- [8] Patel, D. S., and Patel, D. K., Thermal analysis of compound parabolic concentrator. *IJMPERD*, 5, 6, , pp. 117-126, (2015).
- [9] Gnielinski, V., New equations for heat and mass transfer in turbulent pipe and channel flow. *International Chemical Engineering*, (16:2); pp. 359-363, (1976).
- [10] Itoh M., Fujita T., Nishiwaki N. and Hirata M. A, A new method of correlating heat transfer coefficients for natural convection in horizontal cylindrical annuli. *Int. J. Heat Mass Transfer*, 13, pp. 1364-1368(1970).
- [11] Rabl A ., Comparison of solar concentrators. *Solar Energy*, 17, 255, (1976).
- [12] Eames P.C. and Norton B., Detailed parametric analysis of heat transfer in CPC solar energy collectors. *Solar Energy*, 50, 321 (1993).